Journal of Sound and Vibration (1999) **228**(2), 421–441
Article No. jsvi.1999.2412, available online at http://www.idealibrary.com on IDEAL®

CONSTRUCTION OF A PORTABLE TEST RIG TO PERFORM EXPERIMENTAL MODAL ANALYSIS ON MOBILE AGRICULTURAL MACHINERY

P. KENNES, J. ANTHONIS, L. CLIJMANS AND H. RAMON

K.U. Leuven, Faculty of Agricultural and Applied Biological Sciences, Department of Agro-Engineering and Economics, Kardinaal Mercierlaan 92, *B*-3001 *Heverlee, Belgium*

(*Received* 1 *January* 1999, *and in final form* 1 *June* 1999)

Higher working speeds of mobile off-road vehicles arouse dynamical problems like excessive vibrations, which decrease the vehicle lifetime, the driver's comfort, and the working precision. Testing the vibration behaviour of present vehicles is an indispensable source of knowledge for further improvement of vehicle dynamics. More restrictive legislation concerning allowable exposure of drivers to vibrations raises the need for these tests. For small- and medium-sized companies the required know-how and equipment is too expensive and vibration analysis of their products has to be farmed out. Since tests *in situ* have many advantages, a prototype of a mobile low power test rig for experimental modal analysis on vehicles is described in this paper. The vehicle under test is excited vertically under one of its wheels while the other wheels rest on stationary platforms. The power saving by using an airspring parallel to the actuator is investigated by including a model of the airspring in the equations of motion of the test rig. It turned out that the power saving due to the airspring is proportional to the relation of the acceleration due to gravity to the maximum acceleration of the excitation signal. For small band excitation signals extra power savings can be achieved by connection of the airspring with a pressure vessel which optimal size depends on the frequency content of the excitation signal. Experiments with a prototype of the vertical shaker demonstrate that the different modeshapes of a tractor–sprayer combination can be sufficiently excited and modal analysis was performed successfully.

1. INTRODUCTION

All on-road and off-road vehicles are exposed to vibrations caused by unevenness of the road or soil profile, moving elements within the machine or implements. Increased vehicle speed and capacity, induced by higher labour costs, create a lot of vibration problems, reducing the vehicle lifetime, working precision and driver's comfort [1]. This trend is also noticeable for mobile agricultural machinery. Field sprayers are an expressive example of decreasing working efficiency of the equipment due to increasing structural vibrations. Modern self-propelled sprayers have a working width of even more than 40 m, while working speeds in the field up to 4 m/s are no exception. Light sprayer booms with nozzles are used to divide the

0022-460X/99/470421 + 21 $30.00/0

agro-chemicals on the field at a certain dose. Correct application requires a constant height and speed of these nozzles with respect to the ground. Boom oscillations and vibrations are thus disastrous for the homogeneity of the spray liquid distribution on the crop, resulting in under- and over-doses of chemical with a missed treatment effect and remaining residues respectively [2–10]. Driving speed of these spraying machines on the road can reach 40 km/h, which is very high for a vehicle without or with a poor suspension.

High vibration levels between 0·5 and 20 Hz affect also the health of the conductor, especially the backbone is sensitive for severe physical damage in the long term [11–15]. As a consequence several national, European and international standards were established in order to evaluate and restrict the exposition of individuals to vibrations [16–21]. The growing importance of detrimental vibrations on faster machinery arouses the need to evolve from a static design to a dynamic design. To study vehicle dynamics, many analytical methods can be found to build non-linear equations of motion of the system (d'Alembert's principle, method of Newton–Euler, method of Lagrange, Kane's method). They are, however, difficult to solve and require complex vehicle–soil models [22]. Experimental measurement techniques are thus a valuable alternative to study the dynamics of the present-day machinery as a source of knowledge for the state of the art in vehicle dynamics and for the improvement of future machines. Experimental modal analysis originated in offshore-platforms, shipbuilding and aerospace, but penetrated in recent years into agriculture as a means to test tractor and sprayer dynamics [23, 24].

In contrast to the automobile industry most of the agricultural machinery manufacturers are small– or medium–sized enterprises and do not have the know-how and equipment to evaluate the dynamic performance of their machines. Under constraint of more restrictive legislation and higher comfort demands of the clients it is, however, inevitable to measure and reduce the vibration level of their machines. As mentioned, this task will be farmed out to external specialized companies or institutes. Vibration test should be carried out at the commissioning company because of the low mobility of agricultural machinery. Test *in situ* enable furthermore quick adaptations to the tested structure by the manufacturer. This paper deals with the design and prototyping of a new concept for a small mobile shaker to perform experimental modal analysis on mobile agricultural and off-road machinery.

2. PROBLEM: THE EXCITATION DEVICE

Performing an experimental modal analysis on a test structure requires an excitation device providing the input energy to vibrate the test object. The input force is measured by force transducers while accelerometers record the response motions of the structure under test. To study the driving vibrations of vehicles, the input excitation, i.e., soil unevenness, is applied under the wheels. The applied forces can be measured by placing force transducers between the excitator and the wheel.

Within the framework of the European SPECS-project [25] joint measurements were performed on a track simulator at CEMAGREF Montpellier [26, 27] to

build a modal model of a tractor–sprayer combination. The system can reproduce field unevenness under the wheels of a test vehicle by means of seven hydraulic servo-jacks (four vertical servo-jacks to carry the weight of the vehicle and three horizontal ones) driven by a hydraulic power supply of 300 kW. The disadvantage is that the system must be permanently set-up in a warehouse due to its weight and dimensions. Since modal analysis only needs small input displacements to build a modal model, possibilities of a mobile excitation device are examined below.

2.1. CRITERIA FOR THE EXCITATION DEVICE

During the SPECS-project it was proven that an agricultural tractor can be considered as a linear system. The superposition principle allows one to simulate the response of the system for simultaneous inputs under all its wheels by combining modal models built with input excitations alternately under one of the wheels [28]. This permits the use of an excitation device under only one wheel at a time. Linearity of the system allows the use of an excitation device with small amplitudes to build the modal model and to simulate afterwards the responses of the structure for larger input signals. Experiments on the formerly described test rig at CEMAGREF show that 5 cm amplitude is sufficient to excite even the rigid body mode shapes. Since tractor tires act as a low-pass filter, excitation can be limited to the frequency band 0–10 Hz to show all interesting mode shapes [28].

In addition, all important modes of the tractor are controllable from the contact area of any tyre with the soil. This indicates that a simple vertical movement under one wheel can excite all interesting tractor mode shapes. On the other hand, controllability was less for a pure horizontal excitation in lateral or driving direction because of the impossibility to block the wheels perfectly. Moreover, a vertical excitation has the advantage that it can be related to measured or prescribed soil profiles, e.g., ISO 5008 [16].

Based on these findings a prototype mobile shaker is developed to excite a vehicle vertically under one of its wheels with a maximum amplitude of the excitation signal limited to 0·05 m. The main problem for a portable low-power shaker concerns the needed force to lift the tested vehicle, the mass of which can increase up to 40 t for loaded agricultural harvesting machinery. Using a spring parallel to the actuator can compensate gravity and so the needed power can be reduced considerably as shown further on.

2.2. BASIC CONCEPT FOR A PORTABLE SHAKER

As mentioned in the previous section, for experimental modal analysis on a tractor–sprayer combination it is sufficient to excite vertically under one wheel. If the test object is considered as a simple mass (m) on the shaker, the one-degree-of-freedom system can be represented as shown in Figure 1. When the mass is supported by the actuator, the equation of motion is simply:

$$F_{act} = m(\ddot{x} + g), \tag{1}$$

where F_{act} represents the actuator force (N), $\ddot{x}$ is the acceleration of the test object (m/s^2) and g is the acceleration of gravity (m/s^2). Even in static equilibrium the actuator must deliver a force $F_{act} = mg$ to support the test object. In case, the actuator is a hydraulic cylinder supplied by a hydraulic unit, the needed hydraulic power P_{hydr} (W) is

$$P_{hydr} = p_{pump} Q \tag{2}$$

with p_{pump} the pump pressure (N/m^2) and Q the oil flow rate (m^3/s). Since for the position control of the cylinder a constant working pressure p_{const} is required, the hydraulic power is given by

$$P_{hydr} = p_{const} Q = p_{const} A_{act} v_{act}. \tag{3}$$

v_{act} is the velocity of the cylinder (m/s) and A_{act} is the piston working area (m^2). The latter is determined by the maximum force to be delivered (F_{max}) and the working pressure p_{const}:

$$A_{act} = \frac{F_{max}}{p_{const}}. \tag{4}$$

The needed hydraulic power is thus given by

$$P_{hydr} = v_{act} F_{\max}. \tag{5}$$

The actuator speed v_{act} depends on the chosen excitation signal, so the needed maximum actuator force F_{max} determines fully the hydraulic power requirements. According to equation (1) F_{max} can be split in a static part $F_{stat} = mg$ and a dynamic part $F_{dyn} = m\ddot{x}$. For test objects with a large mass as vehicles, the static actuator force represents a considerable part of the needed hydraulic power, especially when the required acceleration of the test object is smaller than the gravity acceleration. The basic idea for the mobile shaker described below is to eliminate this static force

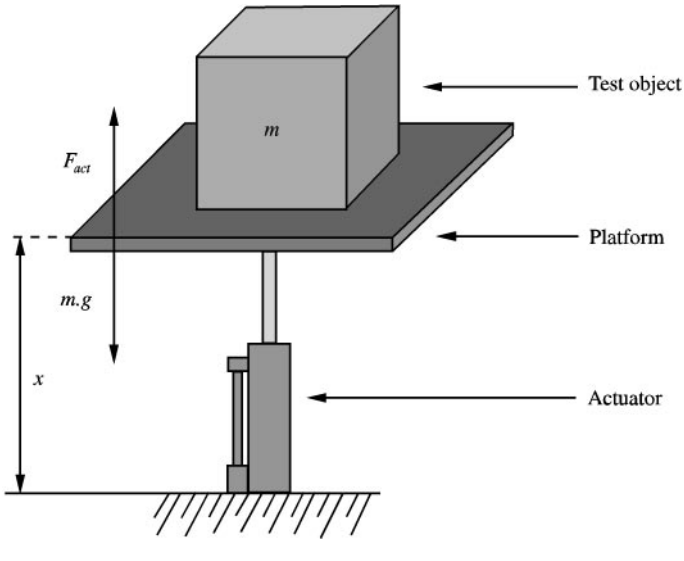

Figure 1. One-degree-of-freedom shaker without parallel spring.

by a spring parallel to the actuator (Figure 2) to enable a reduction of the hydraulic power requirements.

For a shaker with parallel spring, the equation of motion changes to

$$F^*_{act} = k(x - l_0) + m(g + \ddot{x}), \tag{6}$$

where l_0 is the undistorted length (m) of the spring with stiffness k (N/m) (supposed here as constant). In this case, without actuator force the spring will be compressed in static position ($x = x_0$) by a distance d referred to its initial length l_0 given by

$$d = l_0 - x_0 = \frac{mg}{k}. \tag{7}$$

If the test rig is set–up such that in the static position (no actuator force) the actuator is in the middle of its stroke, then the actuator force needed to give the test object a vertical displacement $q = x - x_0$ (Figure 2) equals

$$F^*_{act} = kq + m\ddot{q} \tag{8}$$

as $\ddot{x} = \ddot{q}$ and $x - l_0 = q - d$ in equation (6). Comparison to equation (1) shows that the force required to sustain the test object (mg) is replaced by a force needed to deform the spring (kq). For modal analysis, excitation displacements are small; moreover, if a spring with low stiffness is chosen (see next section), the required actuator force roughly equals the mass inertia of the test object:

$$F^*_{act} \approx m\ddot{q}. \tag{9}$$

The reduction of the necessary actuator force for the shaker with parallel spring compared to a shaker without spring becomes then

$$\frac{F^*_{act}}{F_{act}} = \frac{1}{1 + g/x} \tag{10}$$

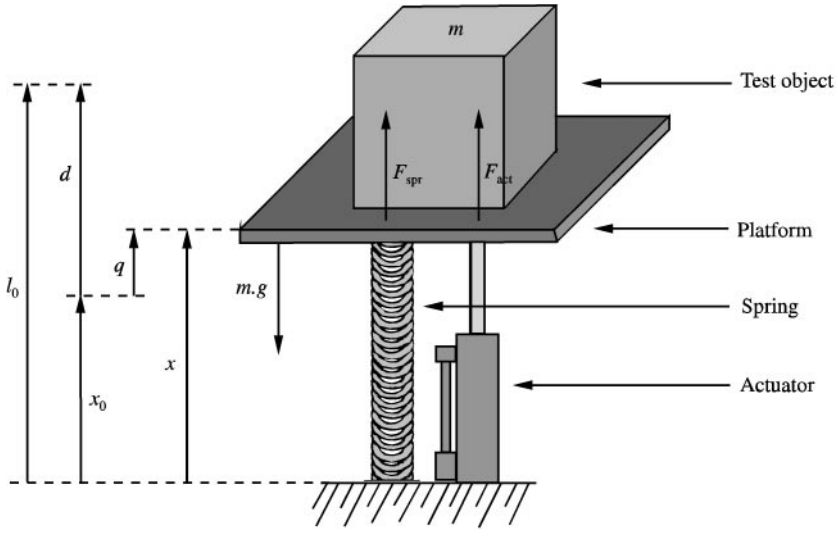

Figure 2. One-degree-of-freedom shaker with parallel spring.

and depends apparently on the maximum applied acceleration of the test object. For accelerations up to 5 m/s^2 for example the force F^*_{act} (with the spring) is only $\frac{1}{3}$th of the force F_{act} (without the spring), so the hydraulic power supply can be reduced by same ratio.

Transformation of equation (8) into the Laplace domain, with s the Laplace variable, yields

$$F^*_{act} = (ms^2 + k)q. \tag{11}$$

Harmonic excitation at the resonance frequency $\sqrt{k/m}$ of the system renders the right-hand side of equation (11) zero and thus, no actuator force is required to excite the mechanism. For a uniform noise spectrum, the larger the spring stiffness k, the larger the required actuator force F^*_{act}. Therefore, a parallel spring with a small stiffness k is recommended. If the applied displacement spectrum for the mechanism has a small band characteristic, k should be tuned such that the zero of $(ms^2 + k)$ coincides with the central frequency of the displacement spectrum. By this the actuator force is minimized. In case of no parallel spring to the actuator, this tuning operation cannot be performed. Consequently, for a shaker without a parallel spring and for a small band displacement spectrum, the required force is not only higher due to the gravity force, but also because of the lack of tuning capacity by which the actuator force F_{act} could be minimized.

2.3. IMPLEMENTATION OF THE PARALLEL SPRING

As mentioned in the previous section, a small spring stiffness k is the best suited for a broadband excitation signal or for a set of different small band signals. For a standard steel compression spring this would require a too long deformation d. An airspring (Figure 3) on the other hand, as employed frequently in suspension of trucks, has a specific sigmoïdal force–compression relation. The isobar

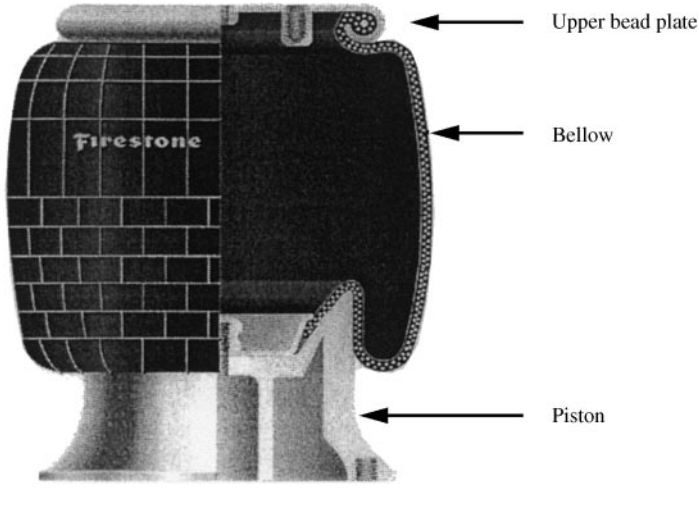

Figure 3. Scheme of airspring (Firestone Airstroke® actuators, Airmount® isolators [29]).

characteristics of the selected airspring (1T14F-2 Firestone Airstroke® actuators, Airmount® isolators [29]) are depicted in Figure 4. In the middle of the airspring's working range (180–280 mm) the curves are almost flat. The chosen airspring allows one to combine a small spring constant with a small mounting height. Care must be taken because these values are only valuable at a constant pressure which can only be realized if the airspring is coupled with a large pressure vessel. For

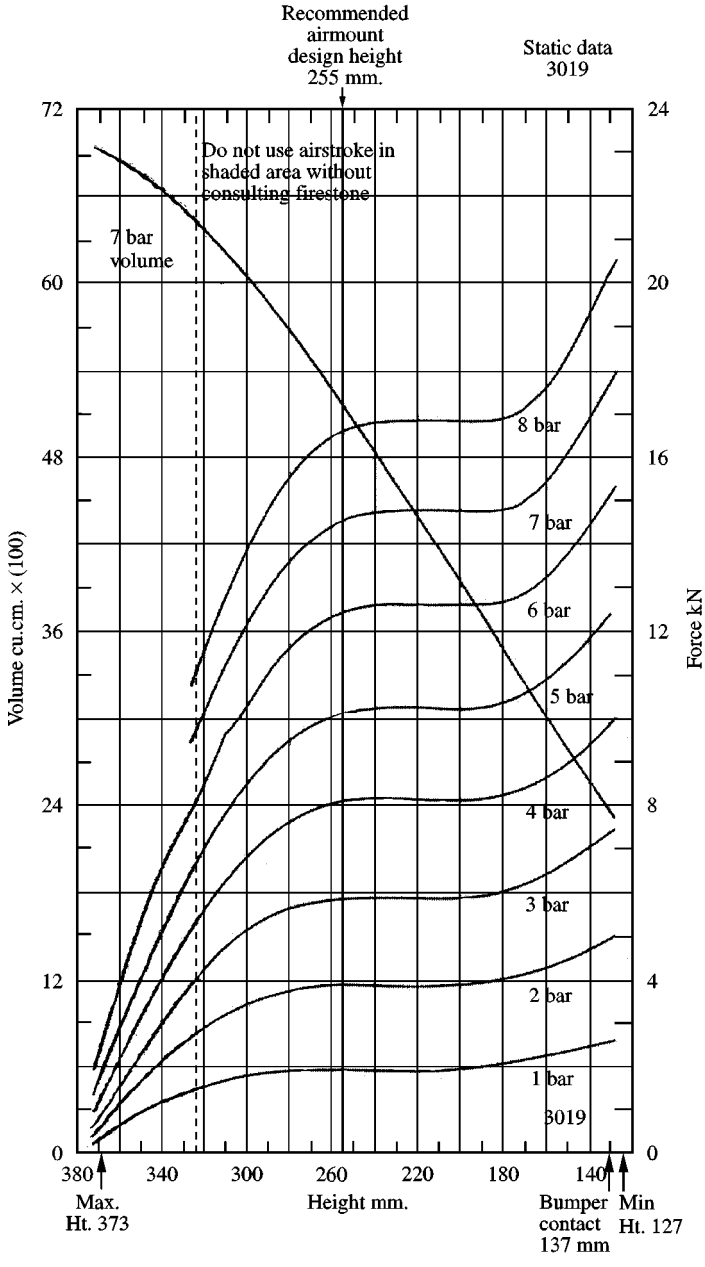

Figure 4. Constant pressure characteristics of an airspring 1T14F-2 (Firestone Airstroke® actuators, Airmount® isolators [29]).

a closed, isolated airspring the pressure variations are not negligible any more and the force–height characteristics are different from the isobar curves, as the measurements shown in Figure 5. The experiments were carried out at six different initial pressures starting from 1 to 6 bar in steps of 1 bar. The initial pressure is measured when the airspring is in the middle of its working range, i.e., at 0·23 m height. The measured curves show hysteresis. However, for small working ranges as for modal analysis, hysteresis becomes insignificant. A second important thing to remark is that in case of a closed airspring the spring constant k is much higher. It is thus possible to reach a desired spring stiffness (as long as it is in between k for the closed airspring and for the isobar curves) by choosing the right pressure tank volume. Therefore, a model of an airspring is developed.

The aim is to derive a relation between the force F_{spr} (N) needed to compress the airspring and its height h(m): $F_{spr} = f(h)$.

The force F_{spr} is given by

$$F_{spr} = p_{spr} A_{spr}, \tag{12}$$

where p_{spr} is the pressure inside the airspring (N/m^2) and A_{spr} the effective area (m^2). The pressure p_{spr} is simply related to the internal air volume V(m^3) as

$$p_{spr} = V^{-1{\cdot}38} m_{air} RT = V^{-1{\cdot}38} c, \tag{13}$$

where m_{air} is to mass of included air (kg), R is the gas constant ($= 288\ J/kg$K for air) and T is the absolute temperature (K) (considered here as a constant). Glancing through the technical data of the airspring established that the air volume V could be approximated as a linear function of the spring height h:

$$V = b_1 + b_2 h. \tag{14}$$

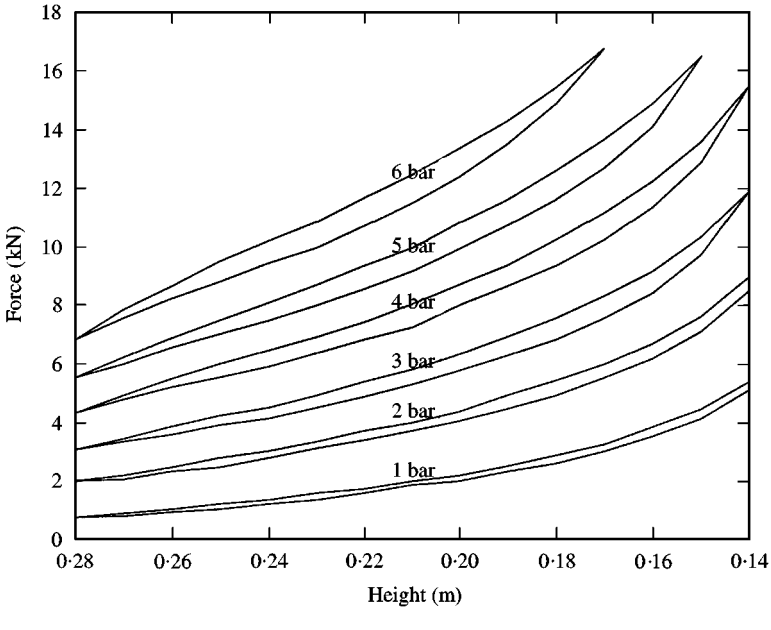

Figure 5. Measured force–position characteristics of a closed airspring Firestone 1T14F-2.

For an airspring connected with an additional pressure tank of volume V_T, the extra volume V_T is added to the right-hand side of equation (14). Combination of equations (13) and (14) give the relation between the internal pressure and the height of the airspring:

$$p_{spr} = f(h) = c(b_1 + b_2 h + V_T)^{-1{\cdot}38}. \tag{15}$$

The only remaining unknown in equation (12) is the effective area A_{spr} which is a function of both the internal pressure p_{spr} and the height h. A third order function in h and a second order function in p_{spr} was selected to approximate this relationship:

$$\begin{aligned} A_{spr} = {} & a_1 + a_2(h + a_9) + a_3(h + a_9)^2 + a_4(h + a_9)^3 + a_5(h + a_9)^3(p_{spr} + a_{10}) \\ & + a_6(p_{spr} + a_{10}) + a_7(p_{spr} + a_{10})^2 + a_8(h + a_9)(p_{spr} + a_{10}). \end{aligned} \tag{16}$$

The parameters a_1 to a_{10} are chosen to approach the effective area values found in the technical specifications as best one can. This is performed by using the "fmin" routine of the Matlab Optimization toolbox. Figure 6 shows the simulated relationship $A_{spr} = f(p_{spr}, h)$ (equation (16)) for an airspring 1T14F-2 (Firestone Airstroke® actuators). The parameters a_1 to a_{10} are in this case: $a_1 = 0{\cdot}0203$, $a_2 = -0{\cdot}0260$, $a_3 = -0{\cdot}7590$, $a_4 = -6{\cdot}7617$, $a_5 = 0{\cdot}4260$, $a_6 = 0{\cdot}0002$, $a_7 = 0{\cdot}0001$, $a_8 = -0{\cdot}0035$, $a_9 = -0{\cdot}255$, $a_{10} = -5 \times 10^5$. The difference between the modelled effective area and the values found in the engineering manual of the airspring is always below 3e-4 m^2, i.e., smaller than 2%.

Combination of equations (12), (15) and (16) gives the demanded relationship:

$$\begin{aligned} F_{spr} = f(h) = {} & c(b_1 + b_2 h + V_T)^{-1{\cdot}38}[a_1 + a_2(h + a_9) + a_3(h + a_9)^2 + a_4(h + a_9)^3 \\ & + a_5(h + a_9)^3\{c(b_1 + b_2 h + V_T)^{-1{\cdot}38} + a_{10}\} \\ & + a_6\{c(b_1 + b_2 h + V_T)^{-1{\cdot}38} + a_{10}\} \\ & + a_7\{c(b_1 + b_2 h + V_T)^{-1{\cdot}38} + a_{10}\}^2 \\ & + a_8(h + a_9)\{c(b_1 + b_2 h + V_T)^{-1{\cdot}38} + a_{10}\}]. \end{aligned} \tag{17}$$

As all parameters a, b and c of equation (17) are determined above, for a given pressure tank volume V_T the force F_{spr} to compress the airspring to a height h can be calculated. Figure 7 shows some simulated force–height characteristics for different tank volumes (0, 1×10^6, 3 and 10 l). Simulation results for a closed air spring ($V_T = 0$) correspond well to the measured force–height characteristics (Figure 5). Connection of the airspring with a fictitious tank of 1000 m^3 renders the isobar curves of Figure 4 (mind the different scales!). Both simulations show that the airspring-model (equation (17)) is able to describe adequately the characteristics of an airspring for different pressures and tank volumes. The other simulations ($V_T = 3$ and 10 l) corroborate the earlier mentioned fact that it is possible to reach a desired stiffness of the airspring (as long as it is in between k for the closed airspring and k for the isobar curves) by choosing the right pressure tank volume. An additional advantage of using an airspring is that the pressure can easily be

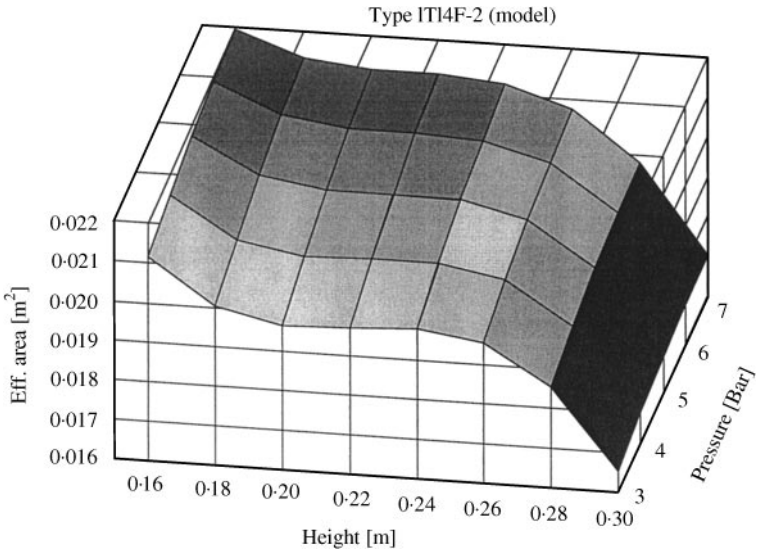

Figure 6. Simulated effective area as a function of pressure and height for Firestone airspring 1T14F-2.

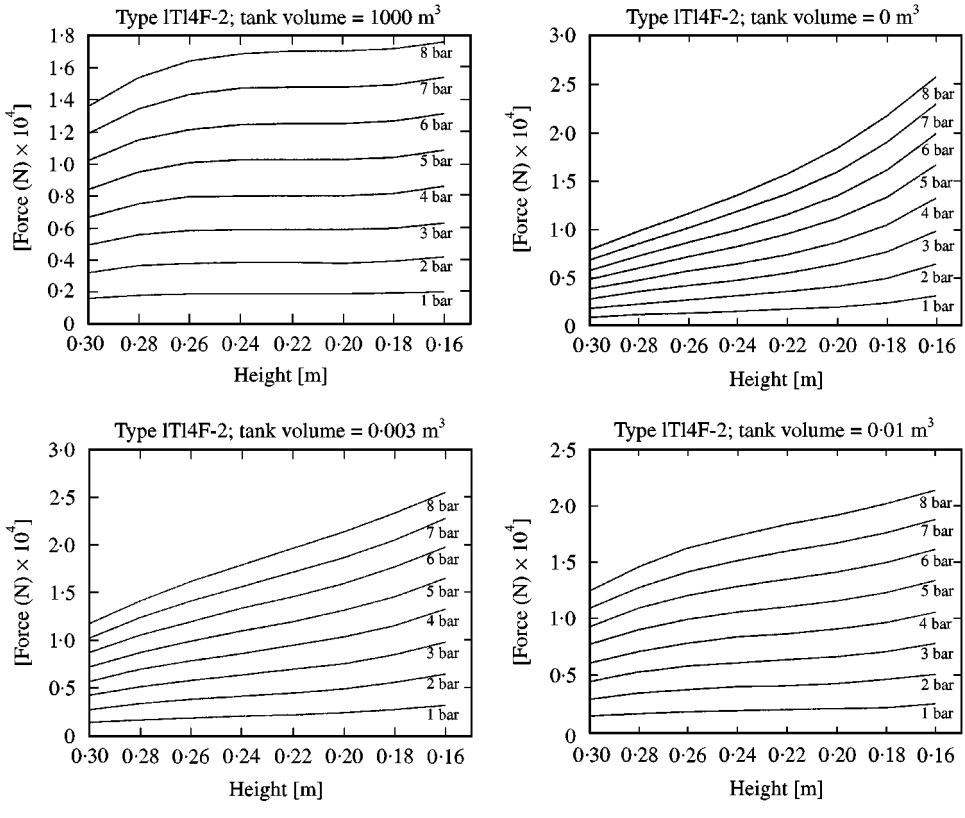

Figure 7. Simulated force–height characteristics for Firestone airspring 1T14F-2 connected to pressure vessel with different volumes (0, 0·003, 0·01 and 1000 m^3).

adapted to the weight of the vehicle on it until the desired height h is reached (while the actuator delivers no force).

3. CONSTRUCTIONAL DETAILS OF THE SHAKER

Figure 8 shows a sketch of the mobile shaker. The height of the platform with the cylinder in its middle position is 0·5 m; its length is 2 m. One of the wheels of the test vehicle is positioned above the airspring. In fact, of the platform movement the platform describes part of a circle around the axis of rotation, but owing to the large radius and limited range of the actuator, it can be considered as a quasi–vertical movement at the rear end where the wheel is placed.

The actuator is a hydraulic double-acting double rod linear cylinder with a total stroke of 0·1 m and a net area of $2{\cdot}9 \times 10^{-4}$ m^2 (Rexroth, type CG 70 E 25/16-XXZ13/01 HFUM11T). It is equipped with a four-way servo-valve (Rexroth, type 4 WS 2 EM6-1 X/5B1ET3157EM) of the critical centre type with a nominal flow rate of 3 l/min at a pressure drop of 70 bar. The power supply consists of an axial displacement pump with adjustable flow rate (14 cm^3/rot), driven by an electro-motor of 11 kW (1500 rot/min). The constant working pressure is set at 100 bar. The hydraulic cylinder is position controlled by an analogue PID controller (Rexroth Servoverstärker VT 1600 S3X) and an LVDT-type distance sensor (Solartron DC 50). As mentioned earlier, a Firestone airspring type 1T14F-2 is used parallel to the actuator. The driving signal is generated on PC and sent via an AD/DA board (Keithley, DAS 1800) to the PID controller either it is sent directly from a wave generator. Figure 9 shows a comparison between imposed displacements (full line) of piston rod with the measured (actual) ones for a swept sine excitation (0·1–10 Hz) when the tractor with mounted sprayer was on the shaker. It can be seen that from frequencies above 4 Hz, the actuator cannot follow the imposed displacements. Nevertheless, enough energy can be brought into the system to perform well a modal analysis test.

Besides the shaking platform, three other tables are used to sustain the other wheels at the same height as the centre position of the movable platform, i.e., 0·5 m (Figure 10). The static tables are connected with each other by an extendable intermediate part, so their relative position can be adapted to the wheel-base of the vehicle under test.

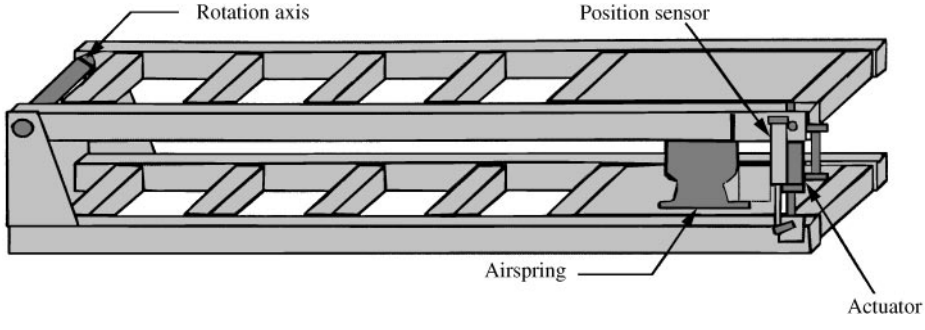

Figure 8. Sketch of the portable shaker.

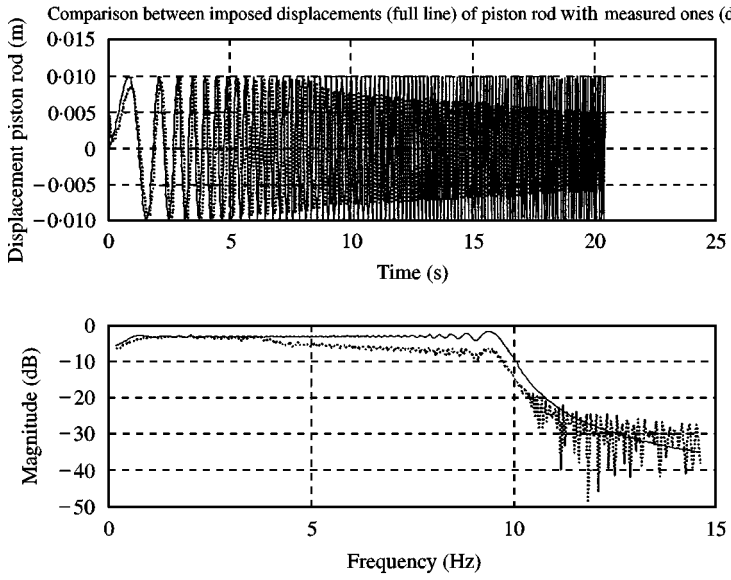

Figure 9. Comparison between imposed displacements (full line) of piston rod with the measured ones for sweptsine (0·1–10 Hz).

4. EXPERIMENTS

Within the framework of the SPECS project the applicability of experimental modal analysis on agricultural field sprayers was examined. The general aim was to characterize the field sprayer's dynamics in the frequency range between 0 and 10 Hz. Higher frequencies are less important because they lead to negligible boom movements, which do not influence the spray pattern adversely. Derived models are used later on for simulation of the boom motions under field conditions in order to calculate resulting dynamic spray liquid depositions.

A survey of the test set-up for experimental modal analysis on a tractor–sprayer combination is given in Figure 11. A portable PC with A/D-D/A plug in board is used both for forwarding the excitation signal to the PID controller of the actuator as for data-acquisition of the response signals from the inductive acceleration transducers (HBM 200) on the tractor or spray boom. The applied input forces at the wheel above the shaking platform are measured by three force transducers sandwiched between the shaker platform and this wheel. Before the response signals from the accelerometers are acquired by the PC, they are signal conditioned (amplification and filtering). After data-acquisition a modal analysis of the structure is performed using LMS CADA-X software.

In the next section, results will be described for tests on an International 845-4WD tractor equipped with a Berthoud sprayer (18 m working width). The tractor is excited under the left rear wheel. Thirty-five measurement points were chosen located on the body of the tractor, the cab, the axles and the motor hood. On each location responses to the input excitations were measured in three perpendicular directions (Figure 12). For the vibration study, a burst random stochastic excitation signal with a spectrum between 0–20 Hz and a length of $\frac{5}{8}$ of

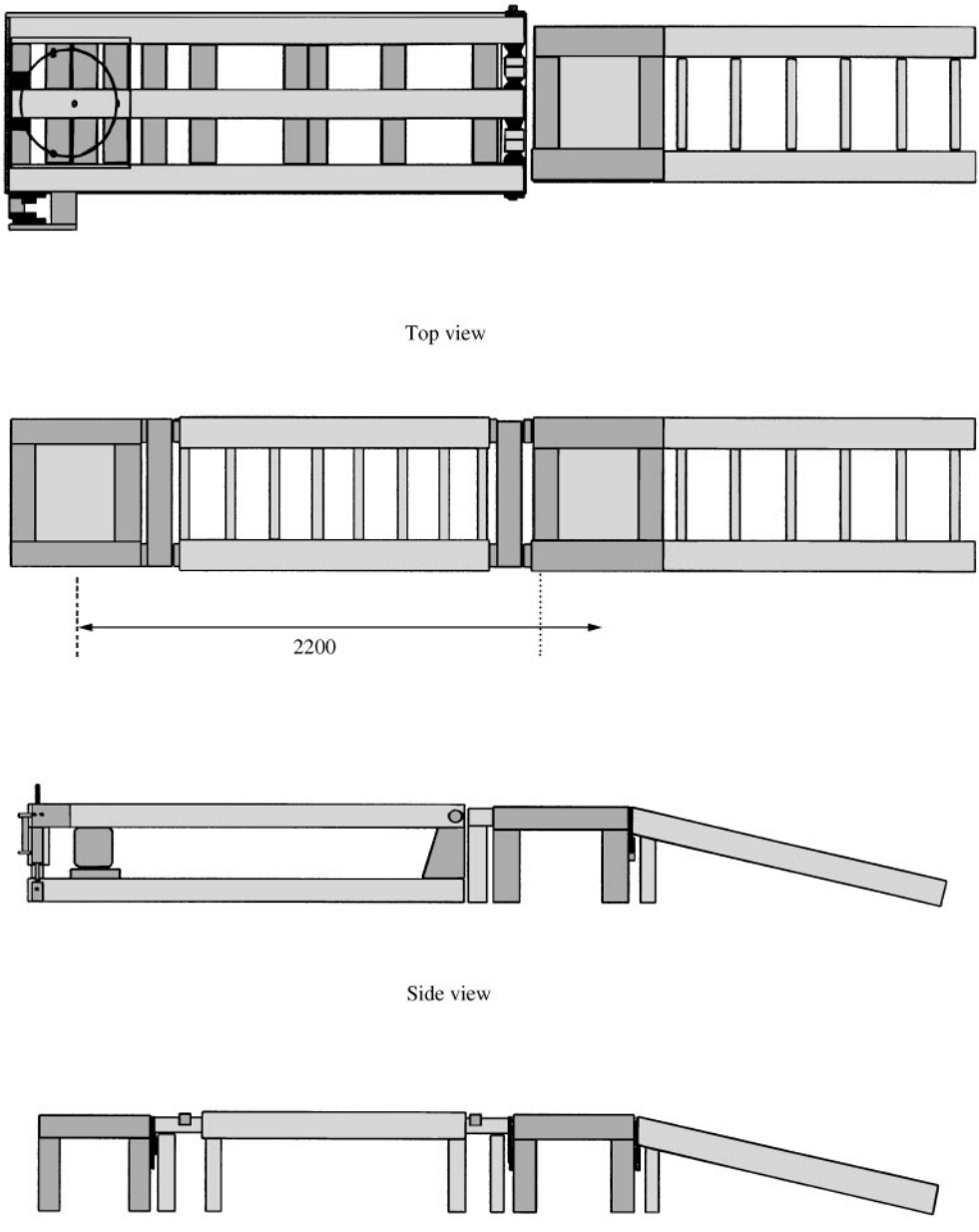

Figure 10. General set-up of the shaker.

the measuring period was used. Because the signals were damped out at the end of the measuring period, no signal windowing was applied. A sampling frequency of 100 Hz and a number of samples equal to 1024, resulted in a measurement time period of 10·24 s and a frequency resolution of 0·097 Hz. An anti-aliasing filter together with an averaging of 20 time periods of the FRFs cancelled out the influence of the noise on the signals. As a result, the coherence between excitation

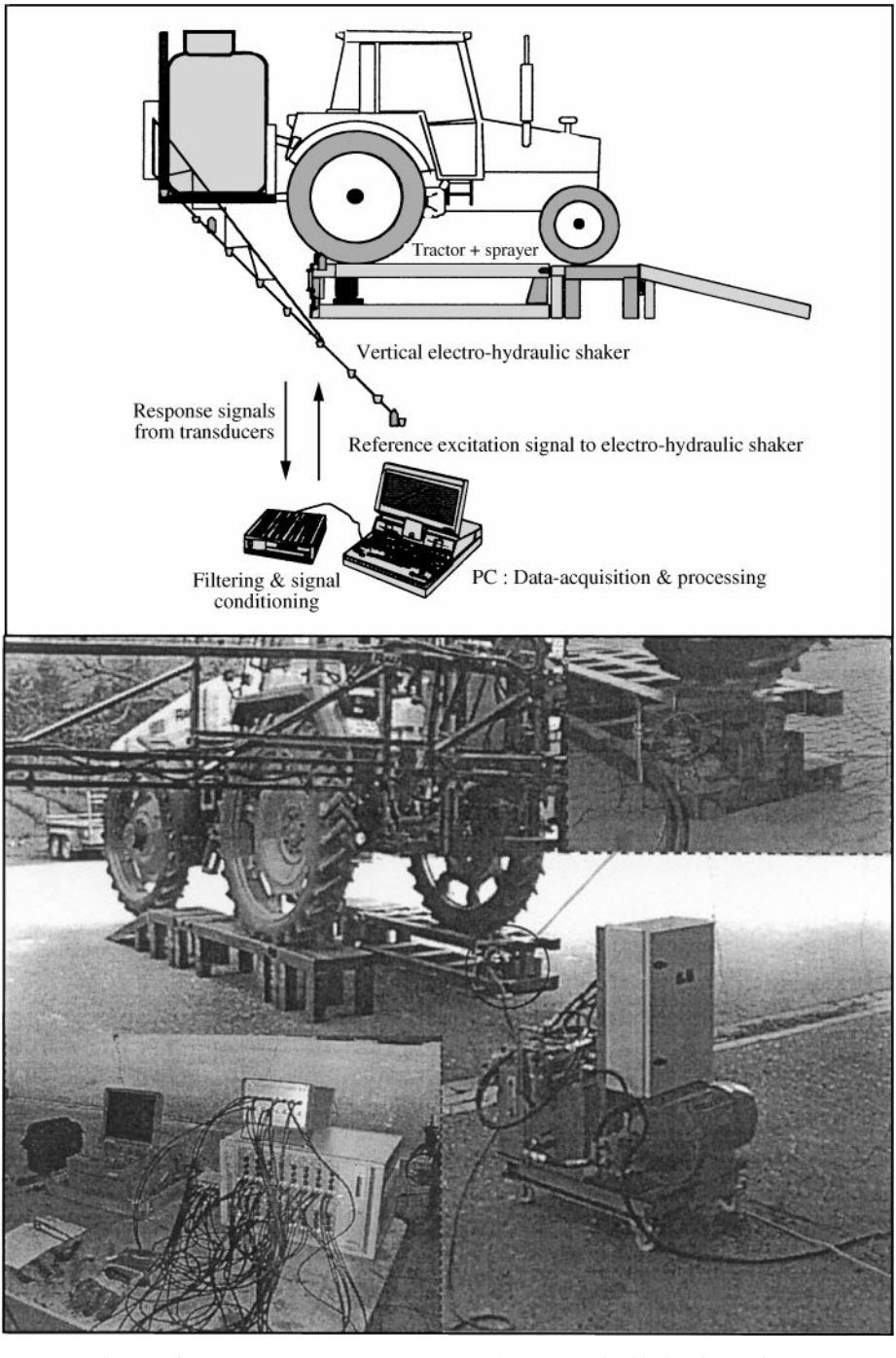

Figure 11. Scheme of the measurement set-up to test the mechanical behaviour of a tractor–sprayer combination.

and response was better than 93%, which ensured the linear behaviour of the tractor. Modal results are depicted in Table 1 and Figures 13–15. The latter represent comparisons between the empirical transfer function estimates (full line)

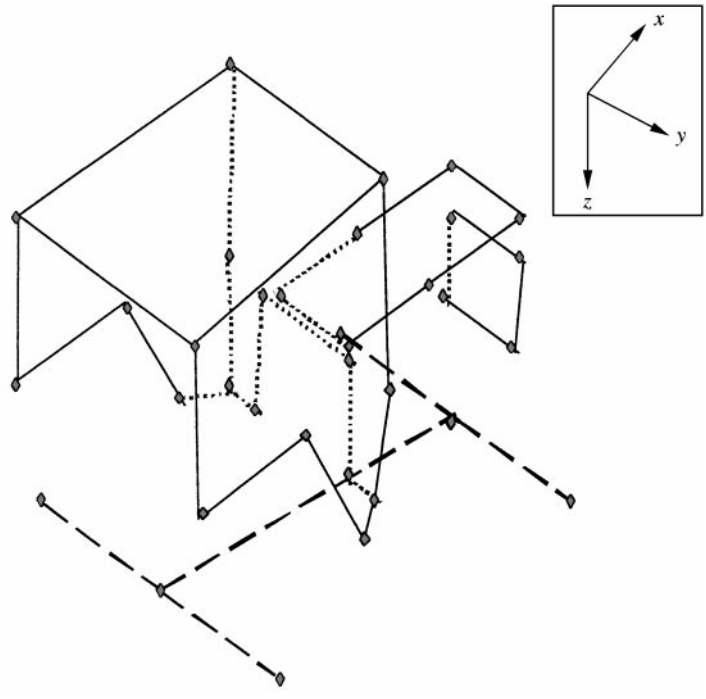

Figure 12. Wire frame representation of measurement points on undistorted tractor.

TABLE 1

Resonance frequencies and corresponding mode participation of tractor (*International* 845-4*WD*)

Mode no.	Frequency (Hz)	Mode participation (%)	Description
1	2·68	21·0	Jump
2	3·06	20·2	Yawing
3	4·27	6·5	Pitching
4	5·05	3·8	Roll
5	6·82	4·3	Cab (local)
6	9·64	17·9	Cab and engine hood (local)

and the transfer function of the model (dotted line) for the right front wheel of the tractor in three perpendicular directions. For all cases, good agreements are obtained between the modelled transfer functions and those estimated from the measured data records.

The wire-frame representation of the sprayer is shown in Figure 16. Special attention is paid to place accelerometers at the hinges that allow to (un)fold the boom since these are crucial places that affect the dynamic behaviour of the boom. A non-periodic stochastic excitation signal in the frequency band 0–6 Hz was used

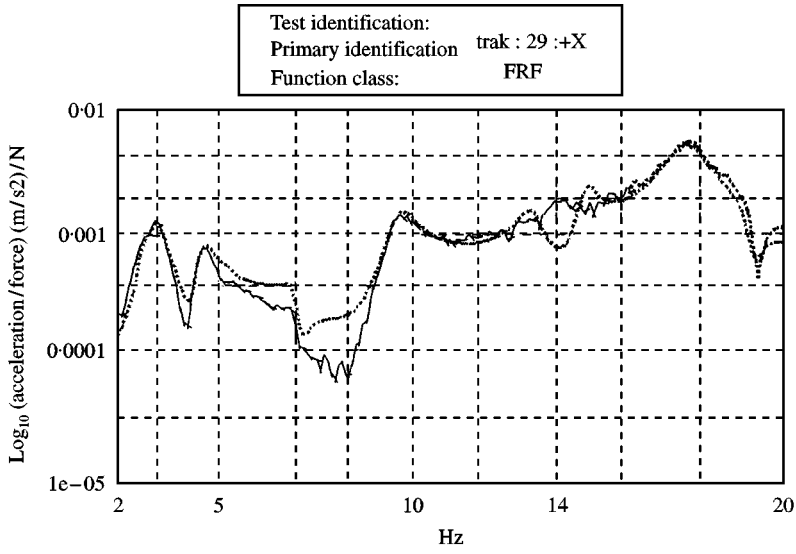

Figure 13. Comparison of FRF synthesized (dotted line) with FRF measured (solid line) for right front wheel of tractor in the transversal direction (correlation coefficient, $r = 0{\cdot}93$). – – –, 0 FRF synthesized; ——, l int_845 FRF Hv-estimator; trak: 29 + X trak: 32 + Z 93% Corr.

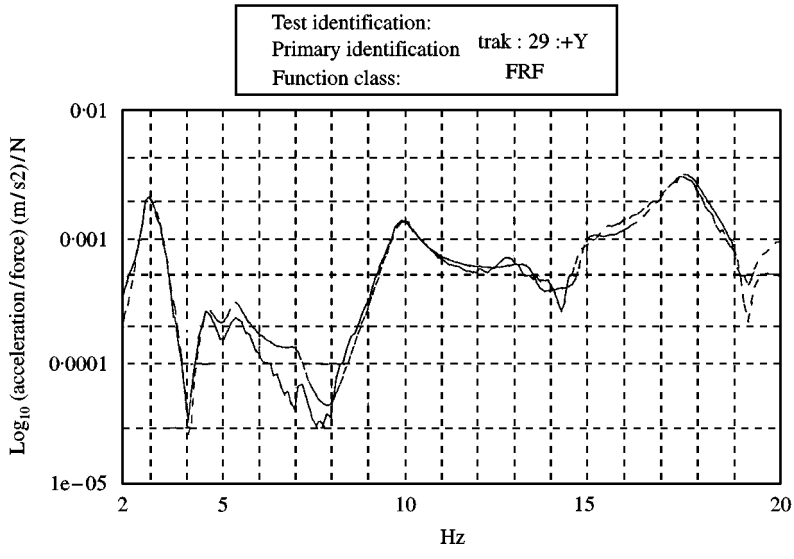

Figure 14. Comparison of FRF synthesized (dotted line) with FRF measured (solid line) for right front wheel of tractor in the longitudinal direction (correlation coefficient, $r = 0{\cdot}95$). – – –, 0 FRF synthesized; ——, l int_845 FRF Hv-estimator; trak: 29 + X trak: 32 + Z 95% Corr.

during this experiment. The captured signals were averaged 30 times and a Hanning window was applied to have as less noise and leakage as possible. Moreover, an overlap of 75% increased the acquisition speed and ensured more reliable results. In this way, a coherence of at least 85% for the different signals was

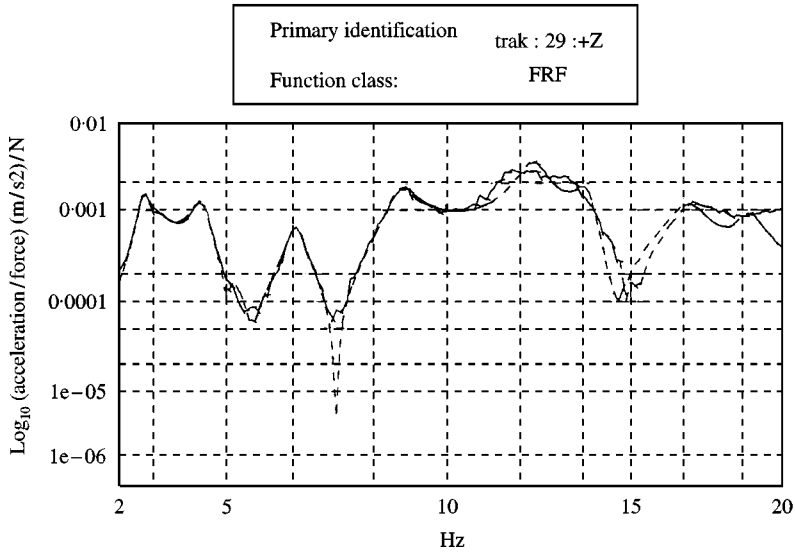

Figure 15. Comparison of FRF synthesized (dotted line) with FRF measured (solid line) for right front wheel of tractor in the vertical direction (correlation coefficient, $r = 0{\cdot}90$). – – –, 0 FRF synthesized; ——, 1 int_845 FRF Hv-estimator; trak: 29 + Z trak: 32 + Z 90% Corr.

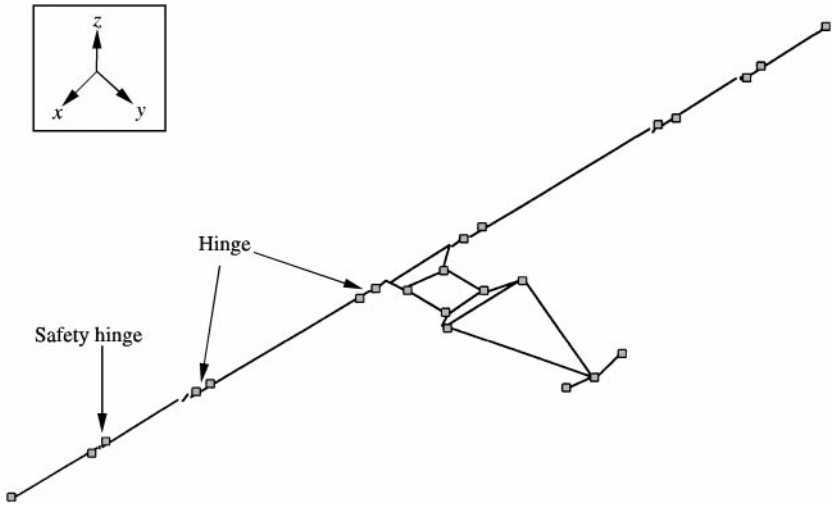

Figure 16. Wire frame representation of measurement points on undistorted sprayer.

attained. Four fundamental horizontal resonance frequencies and three vertical ones and the corresponding mode shapes were found (Table 2). Figures 17 and 18 display the FRFs from the left boom tip for, respectively, longitudinal and vertical direction.

After a modal analysis test the mechanical integrity of operational tractor–sprayer combinations can be evaluated. Defects like worn joints, etc. can easily be detected. This reduces the risk of a breakdown of the machinery at critical

TABLE 2

Resonance frequencies and corresponding mode participation factors for Berthoud sprayer (18 m)

Mode no.	Frequency (Hz)	Mode participation (%)	Description
1	0·73	2·6	Rigid body yawing
2	2·00	1·6	Symmetric 1st flexible mode (hor.)
3	2·44	51·8	Asymmetric 1st flexible mode (hor.)
4	3·71	0·1	Symmetric 2nd flexible mode (hor.)
5	0·73	1·6	Rigid body rolling
6	1·69	1·0	Rigid body jumping
7	2·70	41·3	Symmetric 1st flexible mode (vert.)

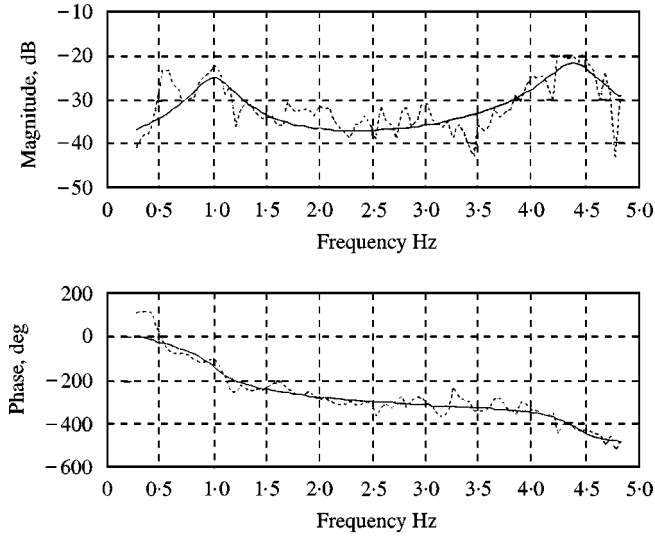

Figure 17. Comparison of FRF synthesized (full line) with FRF measured (dotted line) for left boom tip of sprayer in the longitudinal direction.

moments. Moreover, advice can be granted for mechanical and structural changes based on sensitivity analysis and structural modification predictions.

5. CONCLUSIONS

Incorporating a parallel spring to an actuator allows excitation of even heavy vehicles with a small hydraulic power unit provided that the intended accelerations are not too high. The prototype low-power vertical shaker is able to excite the modes of a tractor–sprayer combination in the frequency-band 0–10 Hz. Supplementary power can be saved for small band excitation signals for which the input force can be minimized by adjusting the stiffness of the airspring (by connecting it with a well-sized pressure tank).

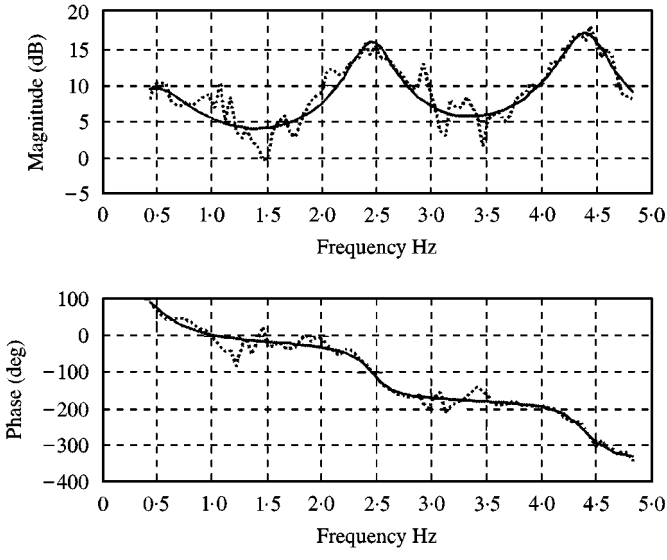

Figure 18. Comparison of FRF synthesized (full line) with FRF measured (dotted line) for left boom tip of sprayer in the vertical direction.

Although the presented shaker with parallel spring is well suited for experimental modal analysis of vehicles, it is not appropriate to perform for example fatigue tests or to reproduce rough tracks. In such cases, large amplitudes and/or accelerations demand a longer stroke of the actuator and huge amounts of power.

ACKNOWLEDGMENT

The authors wish to acknowledge the European Commission for financing the SPECS project.

REFERENCES

1. D. A. Crolla and H. Schwanghart 1992 *Journal of Terramechanics* **29**, 7–17. Vehicle dynamics: steering I.
2. H. Ramon and J. De Baerdemaeker 1997 *Journal of Agricultural Engineering Research* **66**, 23–29. Spray boom motions and spray distribution: Part 1, Derivation of a mathematical relation.
3. H. Ramon, B. Missotten and J. De Baerdemaeker 1997 *Journal of Agricultural Engineering Research* **66**, 31–39. Spray boom motions and spray distribution: Part 2, Experimental validation of the mathematical relation and simulation results.
4. J. Langenakens, H. Ramon and J. De Baerdemaeker 1994 *International Congress for Computer Technology in Agriculture* (*June* 29–*July* 5, *Cambridge*, *UK*). The effect of boom movements on spray distribution.
5. H. Schmidt 1997 *VDI-Tagung* (*Braunschweig*, *Germany*); *VDI Berichte*, 113–116. Simulation und Beurteilung der Verteilung von Pflanzenschutzmitteln beim Einsatz von Feldspritzgeräten (Simulation and assesment of pesticide distribution applicated by field crop sprayers).

6. H. Ganzelmeier and E. Moser 1977 *Grundagen der Landtechnik* **27**(3), 65–72. Einfluss der Auslegerbewegungen von Feldspritzgeraten auf die Verteilgenuigkeit der Spritzflussigkeit (in German).
7. R. B. Rogers, A. Newton and D. R. Menzies 1982 *Meeting American Society of Agricultural Engineers* (*Michigan*). Paper 82-1008. Dynamic behavior of spray booms.
8. L. Speelman and J. W. Jansen 1974 *Journal of Agricultural Engineering Research* **19**, 117–129. The effect of spray boom movements on the liquid distribution of field crops.
9. J. Langenakens, H. Ramon and J. De Baerdemaeker 1994 *The XIIth CIGR World Congress and AgEng*'94 *Conference on Agricultural Engineering* (*August* 29–*September* 1, *Milano*, *Italy*), 1216–1223. The impact of vertical and rolling movements of sprayer booms on the spray distribution.
10. P. Kennes, K. Vermeulen, L. Clijmans and H. Ramon 1998 *IFAC-CAEA*'98 *Control Applications and Ergonomics in Agriculture* (*June* 14–17, *Athens*, *Greece*), 321–325. Comparison of different passive horizontal sprayer boom suspension setups.
11. J. H. van Diën 1993 *Ph.D. thesis Wageningen*, *IMAG-DLO Rapport* 93-5, 150 *pp.* Functional load of the low back.
12. M. L. Magnusson, M. H. Pope, D. G. Wilder and B. Areskoug 1996 *Spine* **21**, 710–717. Are occupational drivers at increased risk for developing musculoskeletal disorders?
13. M. H. Pope and T. H. Hanson 1992 *Clinical Orthopaedics and Related Research* **279**, 49–59. Vibration of the spine and low back pain.
14. W. Christ and H. Dupuis 1966 *Internationale Z Angew Physiol Arbeitsphysiol* **22**, 258. Über die Beanspruchung de Wirbelsäule unter dem Einfluss sinusförmiger und stochastischer Schwingungen (in German).
15. H. C. Boshuizen, P. M. Bongers and C. T. J. Hulshof 1992 *Spine* **17**, 1048–1059. Self-reported back pain in work lift truck and freight container tractor drivers exposed to whole-body vibration.
16. *Norme Internationale ISO* 5008 1979 Tracteurs et matériels agricoles à roues-Mesurage des vibrations transmises globalement au conducteur (in French).
17. *Norme Internationale ISO* 2631/1 1985 Estimation de l' exposition des individues à des vibrations globales du corps—Partie 1: Spécifications générales (in French).
18. *Internationale standard* ISO 5007 1990 Agricultural wheeled tractors—Operator's seat—Laboratory measurement of transmitted vibration.
19. *European Standard EN* 1031 1993 Measurement and evaluation of whole-body vibration—General requirements.
20. *European Standard EN* 1032 1996 Mechanical vibration—Testing of mobile machinery in order to determine the whole-body vibration emission value—General.
21. *European Standard EN* 30326-1 1994 Mechanical vibration—Laboratory method for evaluating vehicle seat vibration—Part 1: Basic requirements (ISO 10326-1: 1992).
22. D. A. Crolla and E. B. Maclaurin 1986 *Journal of Terramechanics* **23**, 1–12. Theoretical and practical aspects of the ride dynamics.
23. L. Clijmans, H. Ramon, J. Langenakens and J. De Baerdemaeker 1996 *Journal of Terramechanics* **33**, 195–208. The influence of tyres on the dynamic behaviour of a lawn mower.
24. L. Clijmans, H. Ramon and J. De Baerdemaeker 1998 *Transactions of the ASAE* **41**, 5–10. Structural modification effects on the dynamic behavior of an agricultural tractor.
25. *SPECS-project* "European system for field sprayer inspection at the farm level". Contract EEC AIR3-CT94-1170.
26. C. Sinfort and B. Bonicelli 1989 *International Congress on Agricultural Engineering* (*Dublin*). Implementation of a vibration test bench for agricultural vehicles.
27. C. Sinfort, A. Miralles, F. Sevila and G. M. Maniere 1994 *Journal of Agricultural Engineering Research* **59**, 245–252. Study and development of a test method for spray boom suspensions.
28. *SPECS-project*, Final Report (1 November '94-30 April '98).

29. Airstroke® actuators, Airmount® isolators, 1994, Firestone Industrial Products Company, 701 Congressional Blvd., Carmel, IN 46032.

APPENDIX: NOMENCLATURE

$a_1, \ldots, a_{10}$	coefficients to approximate A_{spr}
A_{act}	piston working area m^2
A_{spr}	effective area of airspring m^2
b_1, b_2	coefficients that relate V to h
c	constant in gas equation J
d	compression length of spring m
F_{act}	actuator force without parallel spring N
F^*_{act}	actuator force with parallel spring N
F_{dyn}	dynamic actuator force N
F_{max}	maximum actuator force N
F_{spr}	airspring force N
F_{stat}	static actuator force N
g	acceleration of gravity m/s^2
h	height of airspring m
k	spring stiffness N/m
l_0	undistorted spring length m
m	mass of test object kg
m_{air}	mass of air in airspring kg
p_{const}	constant working pressure of hydraulic unit Pa
p_{pump}	pump pressure Pa
p_{spr}	pressure in airspring Pa
P_{hydr}	hydraulic power of hydraulic unit W
q	displacement of test object m
Q	oil flow rate m^3/s
R	gas constant J/(kg K)
s	Laplace variable
T	absolute temperature of air in airspring K
V	internal volume of airspring m^3
V_T	volume of pressure tank m^3
v_{act}	actuator speed m/s
x	actuator position m
$\ddot{x}$	acceleration of test object m/s^2
x_0	static actuator position m